ISSN:1738-6764, eISSN:2093-7504

Advanced LSTM Channel Estimation Scheme in WAVE Communication Systems

Sungmook Lim [1,*]

[1] Department of Electronic Engineering, Korea National University of Transportation; Professor; smlim@ut.ac.kr
* Correspondence

https://doi.org/10.5392/IJoC.2024.20.2.056

Manuscript Received 29 May 2024; Received 25 June 2024; Accepted 26 June 2024

Abstract: *In this paper, in order to overcome the channel distortion due to doubly selective channel, a new deep learning-based channel estimation scheme is proposed. In the proposed scheme, two neural networks are combined to learn both the temporal and spectral characteristics of the channel. One is the AE (autoencoder) which is trained to track the channel characteristic in the time domain and the other is the LSTM (long short term memory) which is trained to track the channel characteristic in the frequency domain. Firstly, the AE is trained and then the LSTM is sequentially trained based on the AE output. After that, the trained neural network is used to the conventional DPA (data pilot aided) process to estimate the channel values in frequency domain. It is noted that the proposed LSTM network consists of fixed number of LSTM units, so it enables to track the temporal variation of the channel reliably, regardless of the position of the OFDM (orthogonal frequency division multiplexing) symbol in a frame. Therefore, the proposed scheme can enhance the PER (packet error rate) performance more by reducing the error propagation due to the DPA process. Through numerical results, it is confirmed that the proposed scheme shows the best PER performance of the conventional schemes in doubly selective channel environment.*

Keywords: Deep Learning; Autoencoder; LSTM; Channel Estimation; WAVE Communication Systems

1. Introduction

As interest in autonomous vehicles increases, many studies are being conducted on V2X (vehicle-to-everything) communication to stably support autonomous vehicles [1]. In particular, IEEE 802.11p/WAVE (Wireless Access for Vehicle Environment) communication systems are being developed to provide V2X communication services [2, 3]. In V2X communication systems with high-speed vehicles, the channel has rapid time-varying as well as frequency selective characteristics, resulting in the performance degradation of V2X systems. Therefore, reliable channel estimation is one of the important challenges to enhance the performance of V2X communication systems.

To overcome the problem, the traditional channel estimation schemes have mainly focused on DPA (data pilot aided) channel estimation schemes. DPA channel estimation schemes update the current channel values by utilizing the demapped data symbols based on the previous channel values as pilots. However, the demapping error causes the performance degradation, so the additional error mitigation process is necessary. In the STA (spectral temporal averaging) scheme, the channel values estimated by the DPA method are finally updated by averaging on both time and frequency domains, resulting in alleviating the performance degradation due to the demapping error [4]. In the TRFI (time domain reliable test frequency domain interpolation) scheme, the reliability test of the estimated channel values is performed where the channel values with low reliability are discarded and updated through the frequency interpolation [5]. Both of them can mitigate channel distortion by introducing the additional error mitigation process after the DPA channel estimation. However, they show the limited performance, especially, as vehicles move faster and the modulation order gets higher.

Recently, the deep learning-based channel estimation methods have been actively researched to drastically enhance the channel estimation performance. In [6], the AE (autoencoder) based channel estimation scheme was proposed, where the AE architecture is introduced to learn the channel characteristics in frequency domain.

It shows the drastic performance enhancement with only three hidden layers and a small number of neurons per a layer, compared with the conventional DPA channel estimation. However, when generating channel data sets used in the training phase, neither the time-varying characteristic of the channel nor the noise in the estimated channel were considered. It limits the channel estimation performance. To overcome this problem, in [7] and [8], STA-DNN (deep neural network) and TRFI-DNN were proposed, where the channel characteristics in frequency domain were trained by DNN, using the channel values estimated by STA and TRFI, respectively. These algorithms consider the noise in the estimated channel, resulting in mitigating the noise due to channel distortion. However, both of them still has the limitation of the performance enhancement, because they do not consider the time-varying characteristic of the channel. In [9], the LSTM-MLP (long short term memory-multiple layer perceptron) based channel estimation scheme was proposed, where the frequency characteristic of the channel was trained by the MLP unit as well as the time characteristic of the channel was trained by the LSTM unit. It shows the better performance than the previous deep learning-based channel estimation schemes, because the time-varying characteristics of the channel is also trained. However, the number of LSTM units is variable according to the position of the OFDM symbol in a frame. When estimating the channel of the i th OFDM (orthogonal frequency division multiplexing) symbol in a frame, i LSTM units are used. When i is small, the learning of the time-varying characteristics of the channel is inaccurate due to the lack of LSTM units. On the other hand, when i is large, the number of LSTM units increases, resulting in too much complexity compared to performance gains. This is a major factor in deteriorating the channel estimation performance despite its high complexity.

In this paper, an advanced LSTM channel estimation scheme is proposed, which can track the channel variation in both time and frequency domains with fixed LSTM units. For this, in the proposed scheme, two artificial neural networks are introduced. The one is AE to learn the frequency characteristics of the channel and the other is LSTM to learn the time characteristics of the channel. In the training phase, we first train the AE with the channel data sets in the frequency domain, subsequently train the LSTM with the data sets trained by the AE. After that, the channel estimates based on the DPA process in each OFDM symbol are updated by using the trained AE-LSTM network. Unlikely the conventional LSTM-MLP, in the proposed scheme, LSTM uses fixed LSTM units, so it can reliably learn the time characteristics of the channel, regardless of position of the OFDM symbol in a frame. When the fixed LSTM units are used, it is important to obtain accurate initial channel values in order to precisely learn the time characteristic of the channel. To overcome this problem, we train the AE first before the LSTM to obtain a possible accurate channel estimates and then use them to train the LSTM. It can enhance the accuracy of the channel estimation and the PER (packet error rate) performance, because the proposed scheme can mitigate the channel distortion and the propagation error due to the DPA process. Through the numerical results, it is confirmed that the proposed scheme outperforms the conventional deep learning-based channel estimation schemes in doubly selective channel environment. In addition, we demonstrate the optimal size of LSTM units to maximize the PER performance.

2. System Model

In this section, we briefly introduce the IEEE 802.11p physical layer structure and the frame structure of WAVE communication systems. The frame structure of WAVE systems is composed of three parts: preamble including short training symbols and long training symbols, signal field and data field. Short and long training symbols are used for time synchronization and initial channel estimation, respectively. Signal field contains the important information for decoding the transmitted data sources such as the modulation order, the coding rate and so on. In the data field, I_{data} OFDM symbols are transmitted, which is variable. Each OFDM symbols contains 64 subcarriers based on 64-point FFT (fast Fourier transform) and IFFT (inverse FFT), which is composed of 12 virtual subcarriers, 4 pilots and 48 data subcarriers. The index sets of virtual, pilot and data subcarriers are defined as $S_V = \{-32,-31,\cdots,-27,0,27,28,\cdots,31\}$, $S_P = \{-21,-7,7,27\}$ and $S_D = S_U \bigcap \left(S_P \bigcup S_V\right)^C$, respectively. S_U is denoted as the total index set, $S_U = \{-32,-31,\cdots,31\}$.

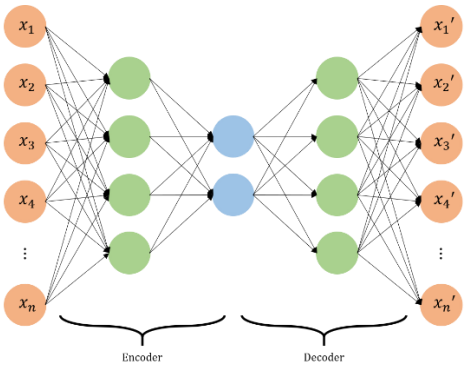

Figure 1. The trained AE structure in AE training phase

The transmitting and the receiving process is as follows. In the transmitter, the original bit information changes into the coded bitstream by the convolutional code, puncturing and interleaving blocks. Then, the demapped symbols are generated by the Mapper. In WAVE systems, BPSK (binary phase shift keying), QPSK (quadrature PSK), 16QAM (quadrature amplitude modulation) and 64QAM are used. After performing 64-point FFT with the demapped symbols and 4 pilot symbols, by adding CP (cyclic prefix), OFDM symbols are generated. Finally, a frame is made by inserting preamble and signal field in front of I_{data} OFDM symbols.

In the receiver, after using short training symbols to find the starting point of the frame and using signal field to obtain the information for decoding, demapping and decoding processes of each OFDM symbol are performed. After performing 64-point FFT, the signal at the k th subcarrier of the i th OFDM symbol, $R_i(k)$, can be expressed as follows:

$$R_i(k) = H_i(k)X_i(k) + N_i(k), \tag{1}$$

where $H_i(k)$, $X_i(k)$ and $N_i(k)$ are the channel coefficient, the data symbol and the AWGN (additive white Gaussian noise) at the k th subcarrier of the i th OFDM symbol, respectively.

Finally, based on DPA process, $X_i(k)$ is demapped by using $H_i(k-1)$, and $H_i(k)$ is estimated and updated, while $X_i(k)$ is considered as data pilot.

3. Proposed Channel Estimation Scheme: Advanced LSTM

In this section, a new channel estimation scheme based on AE-LSM is proposed to enhance the PER performance.

3.1 AE Training Phase

In order to train the proposed AE-LSTM, in the first phase, the AE is trained. Figure 1 shows the trained AE structure. The data set for training is collected from the computer simnulation based on the V2X WAVE simulator. In the V2X WAVE simulator, the transmitter generates each frame based on the IEEE 802.11p physical layer, and then, the signal at the k th subcarrier of the i th OFDM symbol, $R_i(k)$, is received in the receiver. After equalizing and demapping the received signal, the initial channel estimates at the k th subcarrier of the i th OFDM symbol, $\hat{H}_i(k)$, can be expressed as

$$\hat{T}_i(k) = \frac{R_i(k)}{H_{i-1}(k)}, k \in S_D \bigcup S_P, \tag{2}$$

$$\hat{X}_i(k) = Q\left(\hat{T}_i(k)\right), k \in S_D \bigcup S_P, \tag{3}$$

$$\hat{H}_i(k) = \frac{R_i(k)}{\hat{X}_i(k)}, k \in S_D \bigcup S_P, \tag{4}$$

where $\hat{T}_i(k)$ and $\hat{X}_i(k)$ is the equalized signal and the demapped signal at the k th subcarrier of the i th OFDM symbol, respectively, and $Q(\cdot)$ denotes the demapping process. In this process, to obtain the real channel values, we set $SNR = 30dB$ to minimize the noise effect. After that, we generate the input channel data vector $\mathbf{x}_i$ as follows.

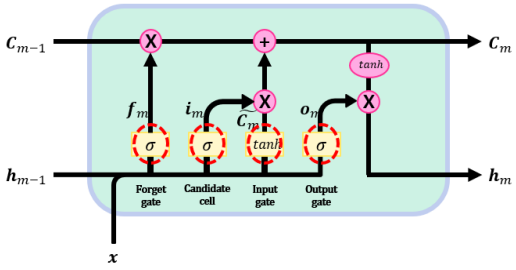

Figure 2. The structure of the m th LSTM unit

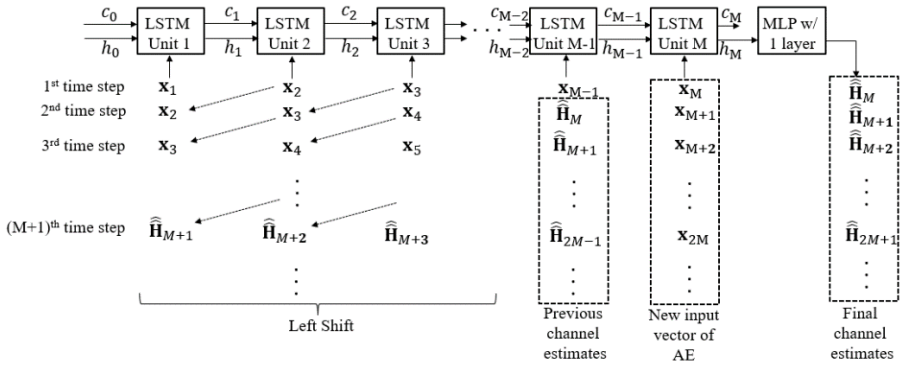

Figure 3. Schematic diagram of the LSTM network

$$\mathbf{x}_\mathbf{i} = \left[real\left(\mathbf{H}_\mathbf{i}\right), imaginary\left(\mathbf{H}_\mathbf{i}\right) \right]^T, \tag{5}$$

where, $[\cdot]^T$ denotes the transpose operation and $\mathbf{H}_\mathbf{i} = \left[\hat{H}_i(k), k \in S_D \bigcup S_P \right]$ represents the i th training channel vector in frequency domain.

By using $\mathbf{x}_\mathbf{i}$ as input data vector, the AE learns the frequency characteristic of the channel. The AE is composed of the encoder and the decoder with L hidden layers. Under the assumption that the AE is fully connected and the dimension of the l th layer is d_l, the output of the l th layer, $\mathbf{h}_l$, can be described as

$$\mathbf{h}_l = \begin{cases} \max\left(\mathbf{W}_l \mathbf{h}_{l-1} + \mathbf{b}_l, 0\right), & l < L \\ \mathbf{W}_l \mathbf{h}_{l-1} + \mathbf{b}_l, & l = L \end{cases}, \tag{6}$$

where, $\mathbf{W}_l$ and $\mathbf{b}_l$ denote the weight matrix with $d_l \times d_{l-1}$ and the bias vector with $d_l \times 1$, respectively. Especially, when $l = 0$, $\mathbf{h}_0$ means $\mathbf{x}_\mathbf{i}$ with $d_0 \times 1$ ($d_0 = 104$). In (6), when $l < L$ and $l = L$, the ReLU (rectified linear unit) and the linear function are used as the activation function, respectively.

Finally, in order to make the output of the AE, $\mathbf{h}_L$, as close to the input vector, $\mathbf{x}_\mathbf{i}$, as possible, parameters of the AE are optimized by minimizing the MSE (mean squared error) as follows.

$$\underset{\{\mathbf{W}_l, \mathbf{b}_l\}_{l=1}^L}{\arg\min} \ \frac{1}{I} \sum_{i=1}^{I} \left| \tilde{\mathbf{x}}_i - \mathbf{x}_i \right|^2, \tag{7}$$

where, $\tilde{\mathbf{x}}_\mathbf{i}$ means the output of the AE, $\mathbf{h}_L$, corresponding as the i th input vector, $\mathbf{x}_\mathbf{i}$ and I denotes the number of training data.

3.2 LSTM Training Phase

In the AE training phase, AE learns the frequency characteristic of the channel and the output of this phase can drastically enhance the PER performance [6]. However, to enhance the PER performance more, we additionally train the temporal characteristic of the channel by using the output of the AE as the input vector of the LSTM in this section.

The structure of LSTM network is shown in Figures 2 and 3. The number of the proposed LSTM network is M , which is fixed and each LSTM unit requires 3 input: the cell state, the hidden state and the input data vector. As shown in Figure 2, the input vector of the m th LSTM unit, $\tilde{\mathbf{x}}_m$, is the output of the AE and the

dimension of which is $2\left(\left|S_D\right|+\left|S_P\right|\right)\times 1$. Based on the cell state, $\mathbf{c}_{m-1}$, the hidden state, $\mathbf{h}_{m-1}$ with $2\left(\left|S_D\right|+\left|S_P\right|\right)\times 1$, and the input vector $\tilde{\mathbf{x}}_m$, the following parameters are updated as

$$\mathbf{f}_m = \sigma\left(\mathbf{W}_f \mathbf{x}_m + \mathbf{U}_f \mathbf{h}_{m-1} + \mathbf{b}_f\right), \tag{8}$$

$$\mathbf{i}_m = \sigma\left(\mathbf{W}_i \mathbf{x}_m + \mathbf{U}_i \mathbf{h}_{m-1} + \mathbf{b}_i\right), \tag{9}$$

$$\tilde{\mathbf{c}}_m = \tanh\left(\mathbf{W}_c \mathbf{x}_m + \mathbf{U}_c \mathbf{h}_{m-1} + \mathbf{b}_c\right), \tag{10}$$

$$\mathbf{o}_m = \sigma\left(\mathbf{W}_o \mathbf{x}_m + \mathbf{U}_o \mathbf{h}_{m-1} + \mathbf{b}_o\right), \tag{11}$$

where $\mathbf{f}_m$, $\mathbf{i}_m$, $\tilde{\mathbf{c}}_m$, and $\mathbf{o}_m$ are the forget gate, input gate, candidate cell and output gate of the LSTM unit with $2\left(\left|S_D\right|+\left|S_P\right|\right)\times 1$. In addition, $\mathbf{W}_j$, $\mathbf{U}_j$ and $\mathbf{b}_j$ ($j \in \{f, i, c, o\}$ are the input weight matrix with $2\left(\left|S_D\right|+\left|S_P\right|\right)\times 2\left(\left|S_D\right|+\left|S_P\right|\right)$, the hidden weight matrix with $2\left(\left|S_D\right|+\left|S_P\right|\right)\times 2\left(\left|S_D\right|+\left|S_P\right|\right)$ and the bias vector with $2\left(\left|S_D\right|+\left|S_P\right|\right)\times 1$ of the forget gate, input gate, candidate cell and output gate according to j, respectively. σ denotes the sigmoid function. Besides, the m th LSTM unit also generates the current cell state, $\mathbf{c}_m$, and hidden state, $\mathbf{h}_m$, as follows:

$$\mathbf{c}_m = \mathbf{f}_m \circ \mathbf{c}_{m-1} + \mathbf{i}_m \circ \tilde{\mathbf{c}}_m, \tag{12}$$

$$\mathbf{h}_m = \mathbf{o}_m \circ \tanh\left(\mathbf{c}_m\right), \tag{13}$$

where $\circ$ denotes the Hadamard product. It is noted that the cell state is to save long-term channel information in time domain, so it plays an important role in obtaining the current hidden state.

Now, let me explain the mechanism of the entire LSTM network with M LSTM units. Unlikely the conventional LSTM-MLP with the variable LSTM units, the LSTM of the proposed scheme has the fixed number of LSTM units. In order to reliably track the channel variation in time domain, the most accurate channel estimates should be used as the first M input vectors of LSTM units. Based on that, we can finally estimate the channel values from the M th OFDM signal in time series by using the proposed LSTM network. For this reason, as shown in Figure 3, in the first time step, $\tilde{\mathbf{x}}_m$ is used as the input vector of the m th LSTM unit ($1 \le m \le M$), and the channel values of the M th OFDM signal in frequency domain, $\hat{\hat{\mathbf{H}}}_M = \left[\hat{\hat{H}}_M(k), k \in S_D \bigcup S_P\right]$, are finally estimated, from the hidden state, $\mathbf{h}_M$. In the second time step, $\tilde{\mathbf{x}}_{m+1}$ is used as the input vector of the m th LSTM unit ($1 \le m \le M-2$) and the final channel estimates in the first step, $\hat{\hat{\mathbf{H}}}_M$, is used as the input vector of the $(M-1)$ th LSTM unit. In addition, $\tilde{\mathbf{x}}_{M+1}$ from the output of the AE is used as the input vector of the M th LSTM unit. It is noted that the input vectors from the first LSTM unit to the $(M-2)$ th LSTM unit are left-shifted from the input vectors from the second LSTM unit to the $(M-1)$ th LSTM unit in the previous time step. It is also noted that the final channel estimates in the previous step is used as the input vector of the M th LSTM unit and the next output vector of the AE is used as the input vector of the $(M+1)$ th LSTM unit. After the $(M+1)$ th time step, all LSTM units except the M th LSTM unit are filled with the previous channel estimates. Because the most accurate channel estimates are used as the input vector of LSTM units in each time step, the proposed LSTM network can learn the temporal characteristic of the channel, resulting in enhancing the PER performance more.

In the proposed LSTM network, in order to finally estimate the channel values in frequency domain, the hidden state of the M th LSTM unit is used as the input vector of the MLP with 1 layer. Then, the output vector of the t th time step, $\hat{\hat{\mathbf{H}}}_{M+t-1}$, can be

$$\hat{\hat{\mathbf{H}}}_{M+t-1} = \mathbf{W}\mathbf{h}_M + \mathbf{b}, \tag{14}$$

where $\mathbf{W}$ and $\mathbf{b}$ is the weight matrix with $2\left(\left|S_D\right|+\left|S_P\right|\right)\times 2\left(\left|S_D\right|+\left|S_P\right|\right)$ and the bias vector with $2\left(\left|S_D\right|+\left|S_P\right|\right)\times 1$ of the MLP, respectively. Based on that, in order to make the output of the LSTM as close to the input vector as possible, $\mathbf{W}$ and $\mathbf{b}$ are optimized by minimizing the MSE (mean squared error), similarly with (7).

3.3 Channel Estimation

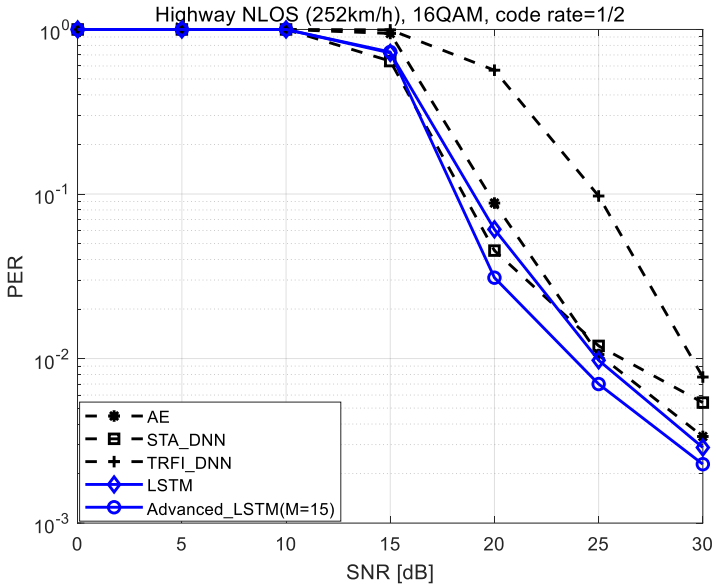

Figure 4. PER performance comparison between the proposed advanced LSTM (M=15) and conventional schemes (Highway NLOS with 252km/h, 16QAM with code rate 1/2)

In order to estimate the channel values in WAVE communication systems, we apply the proposed advanced LSTM network into the DPA channel estimation process. In the receiver, as the first step for the channel estimation, 64-point FFT of the received long training symbols is performed, then the initial channel values at the k th subcarrier can be estimated as

$$\tilde{H}_0(k) = \frac{Y_1(k) + Y_2(k)}{2X_0(k)}, \quad k \in S_D \bigcup S_P \tag{15}$$

where $Y_1(k)$ and $Y_2(k)$ are the first and the second received signals at the k th subcarrier in long training symbols in frequency domain, respectively, and $X_0(k)$ is the training sequence in long training symbols. Based on that, we can estimate the CFRs (channel frequency responses) of the i th OFDM symbol, $\mathbf{H_i} = \left[\hat{H}_i(k), k \in S_D \bigcup S_P\right]$, after equalizing the received signal and demapping the data symbol from (2)-(4).

The estimated CFRs of the i th OFDM symbol, $\mathbf{H_i}$ are fed into the AE's input vector $\mathbf{x_i}$ in (5). It is noted that the output of the AE is $\tilde{\mathbf{x}}_\mathbf{i}$ becomes the final channel estimates when $i \le M-1$. In addition, they are only used as the input vector of the first $(M-1)$ LSTM units in the first time step. On the other hand, when $i \ge M$, $\tilde{\mathbf{x}}_\mathbf{i}$ is fed into the LSTM's input vector of the first M th LSTM unit, and then the final output of the LSTM and the MLP with 1 layer becomes the final channel estimates.

4. Simulation Results

In this section, we compare the PER performance of the proposed channel estimation scheme with the

Table 1. Parameters used in the AE and LSTM training phases

Parameter	Value
Hidden layers in AE	3
Neurons per layer in AE	40-20-40
Number of epochs	400
Batch size	128
Number of epochs	400
Optimizer	Adam
Learning rate, drop period, factor	0.01, 20, 0.8

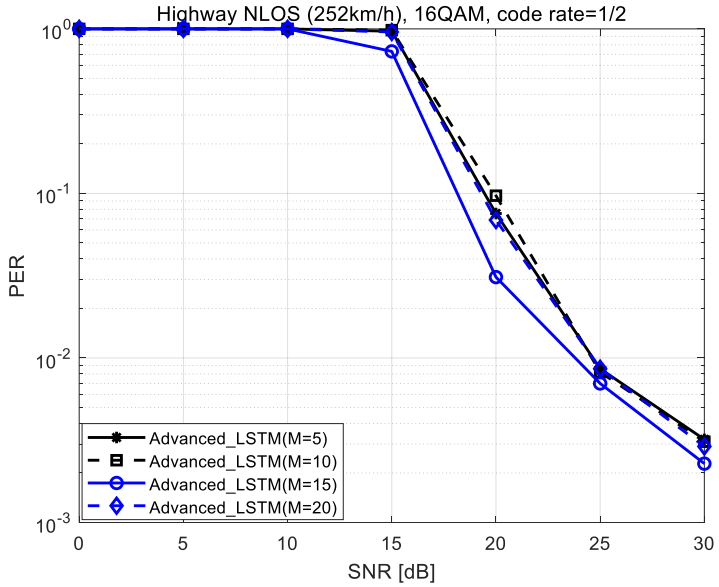

Figure 5. PER performance comparison of the proposed advanced LSTM according to the number of LSTM units (M) (Highway NLOS with 252km/h, 16QAM with code rate 1/2)

conventional schemes and demonstrate the superiority of the proposed scheme. In addition, we discuss the most effective number of the LSTM units through simulation. Cohda wireless channel model is considered, especially '*Highway NLOS (252km/h)*' [10]. The detailed parameters and the channel profile such as Delay and Doppler are listed in [10]. To evaluate the PER performance, 16QAM with coder rate 1/2 is adopted and the number of OFDM symbols in one frame is assumed to be 100. In addition, Table I shows the detailed parameters of the proposed advanced LSTM architecture and those used in the training phase.

Figure 4 shows the PER performance of the proposed advanced LSTM with 10 LSTM units, compared with conventional deep learning-based channel estimation schemes in the channel environment of Highway NLOS with 252km/h. The considered channel is very fluctuated in both time and frequency domains. Therefore, the AE, the STA-DNN and the TRFI-DNN show poor PER performance, because all of them only train the spectral characteristic of the channel. LSTM-MLP shows better performance in a specific SNR region, but its PER performance is similar with the other conventional schemes. It is because the number of the LSTM units in LSTM-MLP is variable, so LSTM unit does not train the temporal characteristic of the channel. In other words, when i is small, the learning of the time-varying characteristics of the channel is inaccurate due to the lack of LSTM units, resulting in degrading the PER performance. On the other hand, it is demonstrated that the PER performance of the proposed scheme outperforms that of the conventional schemes in all SNR regions. It means that the proposed scheme perfectly trains the temporal and the spectral characteristics of the channel based on the most accurate channel vectors, which is important especially in doubly selective channel environment.

In figure 5, according to the number of the LSTM units, the PER performance of the proposed scheme is compared. As the number of the LSTM units increase until M becomes 10, the PER performance is better. The higher the number of the LSTM units is, the more accurate the tracking of the temporal variation of the channel is. However, when M is larger than 10, the PER performance is rather worse. If the number of the LSTM units is too high, the number of the estimated channel values from only the AE without using the LSTM increases, so the opportunity to learn the temporal variation of the channel is lost. In this reason, when $M=10$, the proposed scheme shows the best performance.

5. Conclusions

In this paper, a new deep learning-based channel estimation scheme is proposed in order to overcome the performance degradation due to the doubly selective channel. In the proposed scheme, to learn both the temporal and the spectral variation of the channel, the combined artificial neural network of AE and LSTM is developed. In the first training stage, the AE is trained to learn the spectral characteristic of the channel. And then, in the second training stage, based on the output of the AE, the LSTM is trained to learn the temporal characteristic

of the channel. Especially, by using the fixed LSTM units, it can reliably learn the time characteristics of the channel, regardless of position of the OFDM symbol in a frame. In the channel estimation phase, the trained AE-LSTM network is combined with the DPA channel estimation process. When the number of LSTM units is M, the first M CFRs out of I OFDM symbols are estimated by the AE, on the other hand, the rest CFRs are estimated by both AE and LSTM. The proposed scheme can track the temporal and the spectral variation of the channel, so can enhance the PER performance. It is confirmed that the proposed scheme shows the best PER performance in all SNR regions through numerical results. Also, it is demonstrated that the proposed channel estimation shows the best PER performance when $M = 10$.

Acknowledgments: The research was supported by a grant from the 2022 program for visiting professors overseas in Korea National University of Transportation.

Conflicts of Interest: The authors declare no conflict of interest.

References

[1] K. Zheng, Q. Zheng, H. Yang, L. Zhao, L. Hou and P. Chatzimisios, "Reliable and Efficient Autonomous Driving: The Need for Heterogeneous Vehicular Networks," IEEE Communications Magazine, vol. 53, no. 12, pp. 72-79, Dec. 2015, doi: http://dx.doi.org/10.1109/MCOM.2015.7355569.

[2] A. Ghosh, V. V. Paranthaman, G. Mapp, O. Gemikonakli and J. Loo "Enabling Seamless V2I Communications: Toward Developing Cooperative Automotive Applications in VANET Systems," IEEE Communications Magazine, vol. 53, no. 12, pp. 80-86, Dec. 2015, doi: http://dx.doi.org/10.1109/MCOM.2015.7355570.

[3] IEEE Std. 1609.0-2013, IEEE Guide for Wireless Access in Vehiclular Environments (WAVE)-Architecture, Mar. 2014.

[4] J. A. Fernandez, K. Borries, L. Cheng, B. V. K. Vijaya Kumar, D. D. Stancil, and F. Bai, "Performance of the 802.11p Physical Layer in Vehicle-to-Vehicle Environments," IEEE Trans. Veh. Tech, vol. 61, no. 1, pp. 3-14, Jan. 2012, doi: http://dx.doi.org/10.1109/TVT.2011.2164428.

[5] Y. K. Kim, J. M. Oh, Y. H. Shin, and C. Mun, "Time and Frequency Domain Channel Estimation Scheme for IEEE 802.11p," in Proc. IEEE ITSC'14, Oct. 2014, doi: http://dx.doi.org/10.1109/ITSC.2014.6957832.

[6] S. Han, Y. Oh, and C. Song, "A deep learning based channel estimation scheme for IEEE 802.11p systems," in Proc. IEEE ICC'19, May 2019, doi: http://dx.doi.org/10.1109/ICC.2019.8761354.

[7] A. K. Gizzini, M. Chafii, A. Nimr, and G. Fettweis, "Deep learning based channel estimation schemes for IEEE 802.11p standard," IEEE Access, vol. 8, pp. 113751-113765, Jun. 2020, doi: http://dx.doi.org/10.1109/ACCESS.2020.3003286.

[8] A. K. Gizzini, M. Chafii, A. Nimr, and G. Fettweis, "Joint TRFI and deep learning for vehicular channel estimation," in Proc. IEEE Globecom Workshop'20, Dec. 2020, doi: http://dx.doi.org/10.1109/GCWkshps50303.2020.9367412.

[9] J. Pan, H. Shan, R. Li, Y. Wu, W. Wu, and T. Q. S. Quek "Channel estimation based on deep learning in vehicle-to-everything environments," IEEE Comm. Lett., vol.25, no.6, pp.1891-1895. Jun. 2021, doi: http://dx.doi.org/10.1109/LCOMM.2021.3059922.

[10] Malik Kahn, "IEEE 802.11 Regulatory SC DSRC Coexistence Tiger Team – V2V Radio Channel Models" [PowerPoint Slides] Doc IEEE 80211-14 Feb 2014.